

# **In-Situ Gravimetric Studies of Wetting, Penetration and Wear of Refractories by Molten Slags**

Dongsheng Xie, Ty Tran, and Sharif Jahanshahi

G K Williams Cooperative Research Centre for Extractive Metallurgy  
CSIRO Division of Minerals, Box 312, Clayton South, 3169, Australia

## **ABSTRACT**

Interactions between refractories and slags could involve wetting, penetration, dissolution and structural failure of refractories. Conventional refractory testing techniques, relying on post mortem analysis, provide limited information on the interactive process. To overcome this limitation, a new gravimetric technique, based on wetting and capillary effects, has been developed to provide direct information on dynamic processes of wetting, penetration/dissolution, and wear of the refractories by molten slags.

The technique has been successfully applied to three slag-refractory systems pertinent to typical ferrous and non-ferrous processes. The gravimetric results revealed that the interactions between refractories and slags varied from one system to another, from simultaneous penetration and dissolution, predominant penetration with little dissolution, to severe penetration/cracking and refractory failure due to slag attack.

Characteristics of the wetting and penetration/dissolution were analysed from the gravimetric data. Some important interfacial properties, such as wettability (defined as  $\gamma \cos \theta$ , where  $\gamma$  is surface tension and  $\theta$  the contact angle), and the amount of slag penetration or the net weight change due to penetration and dissolution were estimated. The slag penetration is generally non-uniform and the rate of penetration is influenced by interfacial properties, slag properties and structural characteristics of the refractories. Iron oxide in the slag had a significant effect on wetting and penetration of magnesia based refractories because of its effect on wettability and kinematic viscosity of the slag and its preferential reactions with refractory grains.

# I. INTRODUCTION

Refractory wear due to slag attack is a major concern for many metallurgical processes.<sup>[1,2]</sup> Typical refractory-slag interactions involve sequential steps of wetting, slag penetration, refractory dissolution and structural failure. A good knowledge of these processes is important for our understanding of the mechanisms of refractory wear. Slag attack has been commonly studied<sup>[1,3-6]</sup> by the cup (crucible) test, dip (finger) test, rotary slag test, and induction test. The severity of the slag attack are determined by post-mortem sample analysis, which is inherently tedious and often subjected to human error and interpretations.

To overcome this limitation, a new gravimetric technique has been developed to study the kinetic process of slag-refractory interactions. Based on the principal of wetting and capillary flow, the in-situ gravimetric measurements provide direct information on dynamic wetting, penetration and dissolution of refractories by molten slags. The new technique has been successfully applied to several refractory-slag systems pertinent to typical ferrous and non-ferrous processes. Characteristics of wetting and slag penetration into porous refractories and effect of iron oxide content in the slag were investigated.

# II. EXPERIMENTAL

The experimental set-up is schematically shown in Figure 1. The refractory specimen was suspended above a slag bath and the bottom of the sample made to just contact the surface of the slag contained in a platinum crucible. The weight changes recorded by an electronic balance were logged to a personal computer. The facility was gas-tight to allow control of experimental atmosphere. Argon or other gases were introduced through the gas-enclosed balance box above and passed through a sealed joining tube to enter the furnace. This also served to protect the balance box from excessive heat. Before use, gases were purified to remove traces of moisture and oxygen by passing through a column of silica gel and the copper turning held at 500°C.

The slag was contained in a platinum (10 wt% rhodium) crucible, which sat on an alumina castable platform. The position of the crucible could be adjusted horizontally to allow accurate central alignment of the hanging refractory sample. The crucible and platform were supported by an alumina tube, which passed through a gas-tight hole in the bottom furnace end cap and was securely mounted on a horizontal support arm extending from a linear actuator. The vertical position of the crucible, which was crucial to the weight measurement, was accurately controlled to within  $\pm 0.1$  mm by the linear actuator. Pre-melt synthetic slags of 150-180 g were charged into the crucible (about 70 mm diameter) and the depth of molten slag bath was approximately 13-16 mm.

The cylindrical refractory samples ( $\Phi 20$ -40 mm) were core drilled from bricks. A small hole was drilled at the top of the sample, into which a small diameter alumina tube was cemented coaxially with the cylinder sample using a specially designed alignment tool. Platinum wire was used to connect the small alumina tube to the balance hook. The output of the balance was transferred to a personal computer, and the data could be logged at speeds as high as 5 readings per second to

give sufficient data points for analysis, particularly during the initial contact period. The accuracy of the balance was 0.1 mg.

The procedure of the experiments was as follows. After the refractory sample was carefully aligned and positioned within 10-20 mm from the surface of the pre-melted slag held in the crucible, the furnace and its contents were heated to desired temperature under a controlled gas atmosphere (eg argon). The logging of the balance reading was then initiated and the crucible was raised slowly until contact with the refractory sample was made. This was observed by a sharp increase in the balance weight reading (this applied to all systems where the slag wetted the refractory samples). The weight changes were continuously recorded over the desired period of the slag-refractory contact, which varied from about 40 min to 2 hours depending on the system. At the end of the gravimetric measurements, the crucible was lowered until the slag contact with the refractory sample was ceased. Immediately after this, the refractory sample was raised about 200 mm into the cooler zone of the furnace, in order to freeze the slag soaked inside the sample. After the furnace was cooled to room temperature, the samples were removed and photographed. The samples were then sectioned and analysed for the chemical composition using XRF and examined using SEM or microprobe techniques.

### III. RESULTS

Three slag-refractory systems were studied. In the first case, interactions between a silicate slag in the system of  $\text{CaO-SiO}_2\text{-Al}_2\text{O}_3\text{-MgO}$  and a magnesia spinel brick were studied and effect of refractory sample size and addition of 5 wt%  $\text{FeO}_x$  in the slag were investigated. Studies on a second model system investigated attack by a calcium ferrite type slag on a magnesite and a magchrome brick. In the last case, attack by a ladle type slag on four alumina castable refractories was investigated. The experimental results are described in details below.

#### *A. Silicate Slag and Magnesia Spinel Refractory*

The chemical compositions of the refractory and slag are listed in Table 1. The refractory was a magnesia spinel brick (added  $\text{MgO}\cdot\text{Al}_2\text{O}_3$  spinel shown in Table 1 as alumina) and three cylindrical samples were used with diameters of 20, 30 and 40 mm. About 150 g of the synthetic slags were used for each experiment. The experiments were conducted at 1500 °C under argon and the slag-refractory contact time was about 40 minutes. The gravimetric curves obtained and the photographs of the refractory samples after the tests are shown in Figure 2. The results showed that the silicate slag penetrated extensively into the refractory and, simultaneously, the refractory was dissolved into the slag, particularly at the slag contact level (showing typical necking and slag line corrosion due to the Marangoni effect).<sup>[7,8]</sup> The bottom of the sample was also attacked severely and showed “crater” shaped corrosion, which is also believed to be caused by Marangoni flow.<sup>[9]</sup> Creeping of the slag on the refractory sample wall was apparent for all samples, the height of the creeping layer being approximately same (15 mm), irrespective of sample size.

Effect of addition of 5 wt%  $\text{FeO}_x$  to the silicate slag was studied using a 30 mm sample under identical experimental conditions as above. The gravimetric curves and tested refractory samples

are shown in Figure 3 in comparison with those for the slag without any  $\text{FeO}_x$ . The addition of 5 wt%  $\text{FeO}_x$  significantly enhanced the penetration as evidenced by the prolonged net weight gain over two hours. The sectioned samples (after the test) clearly showed darker areas penetrated by the iron oxide containing slag.

### *B. Calcium Ferrite Slag - Magnesite or Magchrome Refractories*

The interactions of a magnesite and a magchrome refractory with a calcium ferrite type slag were investigated. The chemical compositions of the refractories and the slag are shown in Table 2. The  $\text{MgO}$  refractory was a magnesite brick, which was different from the previous magnesite spinel brick. Refractory samples were 30 mm in diameter and 44 mm in height. About 120 g slag samples were used. The experiments were conducted at 1300 °C and an oxygen partial pressure of  $10^{-6}$  atm, controlled using a  $\text{CO}_2$ -CO mixture. The refractory-slag contact time was 1-2 hours. The gravimetric curves and the photographs of the samples before and after the test are shown in Figure 4.

The sectioned samples after the tests showed extensive penetration in both types of refractories, particularly the  $\text{MgO}$  refractory. This was also indicated by the bright slag-soaked sample surface (Figure 4). The penetration in the  $\text{MgO}$  refractory was so severe that the slag almost soaked the entire sample after 2 hours of contact. Both samples did not show any substantial slag line corrosion. At the end of the tests, the slag composition was almost unchanged and the slag weight loss was, within the experimental uncertainty, equal to the sample weight gain. Therefore, the gravimetric data (after correction of wetting as discussed later) could be used directly as a measure for the penetration of the slag. It is interesting to note that the penetration in the magchrome refractory was initially very fast but slowed dramatically after about 10 minutes and almost ceased after about 15 minutes. The sectioned sample showed a slag penetration front at about 32-34 mm from the hot face (slag-refractory contact).

### *C. Ladle Slags - Alumina Castable Refractories*

Four alumina-based castable refractories were tested against a ladle type slag. The chemical compositions of the refractories and the slag are listed in Table 3. These alumina castables were produced by different manufacturers for steel ladle applications. Following the recommended procedures by the manufacturer, the castable mixes were cast into bricks and then fired. Cylindrical samples of 30 mm diameter were then core drilled from the fired bricks. The length of the four castables was different from one other (specified later in Figure 5) as some were obtained from large precast blocks for use by rotary slag tests. The experiments were conducted at 1600 °C under argon and approximately 150 g of pre-melted slag was used. The slag-refractory contact time was 2 hours. The gravimetric curves and the photographs of the tested refractory samples are shown in Figure 5.

Considerable difference in slag attack was found among the four castable refractories. At the end of the experiments, the refractory samples had weight losses from 3 to 11 g and showed penetration of the slag to a varying degree. Castables B and D were least penetrated (or dissolved) by the slag, and the weight losses were much less than the other two castables, showing a higher resistance to the slag. In comparison, Castables A and C were severely attacked

by the slag, due to extensive penetration and considerable dissolution/spalling of refractory grains. It is interesting to note that the apparent attack on Castable A appeared to occur mainly through internal penetration while the slag attack on Castable C was more severe in the surface region causing expansion and cracking. The gravimetric curves for Castable C showed that the slag attack occurred almost immediately after the refractory contacted the slag, while the rapid rise, and subsequent decrease in the gravimetric curve, was likely to be due to the cracking or spalling of the refractory grains.

## IV. DISCUSSIONS

### *A. In-Situ Gravimetric Technique*

The in-situ gravimetric curves relate to well defined physical processes as illustrated in Figure 6. The sharp weight increase at the initial slag-refractory contact was due to the wetting by the slag and the slag surface tension, exerting a “pull” on the cylindrical sample. The weight changes after initial contact showed the net effect of two simultaneous processes: slag penetration and refractory dissolution. The weight gain in the early stage resulted from greater slag penetration than slag dissolution. The rate of penetration would decrease as the slag penetrated deeper, and the weight gain would eventually be expected to reach a maximum at which the rate of dissolution was equal to (and then exceeded) that of slag penetration.

The relative importance of slag penetration or dissolution processes, and indeed other radical weight changes observed, depended on the slag-refractory system studied and varied from one system to another. For the magnesia spinel refractory and silicate slags (Figures 2 and 3), the gravimetric curves showed simultaneous penetration and dissolution similarly to that in Figure 6. For calcium ferrite slags in contact with the magnesia and magchrome refractories, the gravimetric curves showed fast and extensive penetration with little dissolution (Figure 4). In the case of the ladle slag with four alumina castables, mixed behaviours were observed and severe attack and dissolution by ladle slags occurred in some cases (Figure 5).

A significant advantage of the new gravimetric technique is its capability to provide in-situ kinetic information on the whole process of the slag-refractory interactions from the initial contact, to severe slag attack and refractory failure. In particular, in-situ measurements provide direct insights into refractory wear due to fast and instantaneous reactions, such as cracking and spalling in some alumina castables when attacked by the ladle slag (Figure 5) and the rapid penetration of calcium ferrite slags into the magnesia and magchrome refractories (Figure 4). Such information is difficult, if not impossible, to get from existing conventional techniques based on post-mortem analysis.

It is beyond the scope of the present publication to provide a comprehensive analysis of slag-refractory reactions and wear mechanisms in the foregoing three model systems. Detailed analysis of gravimetric results obtained and the microscopic examination of the samples tested will be the subject of future publications. The following discussions are focused on the interpretation of gravimetric data in relation to the characteristics of wetting and slag penetration.

## B. Wetting and Interfacial Properties

Figure 7 showed the gravimetric curves for the first 20 seconds after contact was made between the magnesia spinel refractory and the silicate slag (Figures 2 and 3). Obviously, establishment of initial contact was very fast and this was immediately followed by very fast penetration, shown by a rapid weight increase for up to about 4 seconds, when the rate of weight gain then slowed.

The surface tension of the slags may be calculated from the initial weight increase (between free-hanging sample and slag wetted sample) if the non-smoothness of the porous refractory surface was ignored and initial fast penetration could be estimated. The first assumption was reasonable as the pores in the refractory were generally very small (median pore sizes around 10  $\mu\text{m}$ ) and liquid contact at such a surface would tend to smoothen out and form a continuous meniscus similar to that formed at a smooth cylinder bottom. To correct the contribution from the initial fast penetration, the gravity and wetting force (estimated from the apparent weight) per unit contact length of nominal circumference ( $F$ ,  $\text{dyn cm}^{-1}$ ) measured at 4 sec was plotted as a function of the nominal contact area ( $A$ ,  $\text{cm}^2$ ) as shown in Figure 8. A linear dependence is observed, within the experimental uncertainties, and expressed by the equation:

$$F = 423.5 + 38.35A \quad (1)$$

The second term represented the contribution of fast penetration which was proportional to the contact area. Extrapolating to zero contact area gives an  $F$  value of 423  $\text{dyn cm}^{-1}$ . If the non-smoothness of the cylinder circumference is ignored, this should be equal to  $\gamma \cos\theta$  where  $\gamma$  is the surface tension of the slag and  $\theta$  is the contact angle at the slag and refractory contact. The term  $\gamma \cos\theta$  is an important measure of wetting characteristics and has been referred<sup>[10]</sup> to as “wettability parameter” or simply “wettability” (which will be used hereafter).

The surface tension of the silicate slag used has not been measured. However, extrapolation from the published surface tension data for similar systems<sup>[11,12]</sup> gives a value of  $\gamma \approx 430 \text{ dyn cm}^{-1}$ . No data is available for the contact angle but it may be reasonably assumed to be small and hence  $\cos\theta$  should be close to unity. This leads to  $\gamma \cos\theta \approx 430 \text{ dyn cm}^{-1}$ , in close agreement with that estimated from the gravimetric results. Figure 7 also showed the gravimetric curve for the slag with addition of 5 wt% “ $\text{FeO}_x$ ”. Using Eq (1) to correct the initial fast penetration, the estimated value for  $\gamma \cos\theta$  was  $\sim 429 \text{ dyn cm}^{-1}$ , slightly higher than that for the slag without iron oxide.

The gravimetric curves for the calcium ferrite slag with the magnesia and magchrome refractories in the first 20 seconds are presented in Figure 9. The initial weight increase was much higher than those observed for the silicate slags with the magnesia spinel refractory. The properties of the calcium ferrite slags differed significantly from those of the silicate slags so Eq (1) was not applicable. However, as there was little dissolution from both refractories, and the samples retained their original cylinder shape at the end of the tests, the weight changes prior to, and after the slag separation from the refractory sample at the end of the tests, may be used to estimate the wettability. Loss of a substantial amount of the slag due to penetration caused a drop in the slag surface and resulted in a slag film between the slag bath and the refractory sample before its break-up. This was corrected for based on the known density of the slag.<sup>[13,14]</sup> The estimated wettability values were 608 and 523  $\text{dyn cm}^{-1}$  for magnesia and magchrome, respectively. This is broadly consistent, assuming  $\cos\theta \approx 1$ , with literature surface tension values<sup>[12]</sup> of 520-630  $\text{dyn}$

cm<sup>-1</sup> for similar slags at 1350°C. The difference in estimated  $\gamma \cdot \cos\theta$  between the two refractories appears to be likely due to the different wetting contacts rather than caused by the experimental uncertainties. If we assume  $\theta = 0^\circ$  for the magnesia refractory, the slag contact angle at the magchrome surface would be approximately 30°.

### *C. Penetration of Slags*

The penetration of the slags into the refractories is a complex process and is generally non-uniform in nature. The penetration front does not usually show as a clear-cut boundary, and very often rather as a blurred boundary region. In the areas which have been penetrated, not all pores are filled with the slag and the slag penetration through interconnected pores followed selective channels and pathways. This makes it difficult to quantify the true depth of penetration. Obviously any such depth should be treated as an average whether it is determined by the amount (weight) of the slag penetrated, or by virtual microscopic examination.

The present design of the slag-refractory contact is quite unique benefiting from the gravimetric technique which allows accurate control of the contact position. This helps to restrict the mass flow across a well-defined contact area in one direction. In comparison, conventional techniques such as the “finger” test commonly use a partly “immersed” sample<sup>[15]</sup> which complicates the conditions for data analysis and interpretation.

For refractory-slag systems without apparent slag creeping on the surface, the penetration of the slag could be estimated based on the gravimetric data after correction of the wettability and the weight of the slag film, if not negligible, at the slag-refractory contact. Applying to the calcium ferrite slag with the magnesia and magchrome refractories, the amount of the penetrated slag was estimated and is shown in Figure 10 as a function of contact time. Two short horizontal bars at the end of each curve indicated the net weight gain by the refractory sample measured from the free hanging sample after the slag-refractory contact was ceased. It is interesting to note that the rate of penetration was almost same for both refractories during the first 13 minutes. As discussed previously, the wettability ( $\gamma \cdot \cos\theta$ ) for the magnesia refractory was likely to be higher than for the magchrome, thus predicting a faster penetration of slag if other properties were identical. Lower wettability for the magchrome refractory, however, was compensated by a higher porosity (about 20%) and a relatively larger median pore size (~ 10.5  $\mu\text{m}$ ) in comparison with the magnesia refractory (about 16% and 6.8  $\mu\text{m}$ , respectively). The levelling off of penetration curve at longer period for the magchrome refractory was probably due to the reactions between penetrated slag and refractory grains, causing changes in the composition and hence properties of the slag (such as melting temperature). Visual examination and chemical analysis of the sectioned sample indicated the penetration front to be as deep as 34 mm, which was higher than that estimated (~ 25 mm), if all pores had been filled by the slag. Apparently, some pores, particularly in the areas close to the front, were unfilled.

Slag creeping provides possible alternative routes for slag to enter the refractory, and thus complicates the conditions. Creeping was observed when the silicate slag contacted the magnesia spinel refractory. The height of creeping on the cylinder surface was about 15 mm for all refractory samples of variable diameters. As the experiment using 5 wt% FeO<sub>x</sub> slag ran for 2 hours, compared with 40 minutes for the slags without iron oxide, the observation of no

difference in the creeping height suggested that the creeping reached that height probably in a relatively short time. To estimate its contribution, the gravimetric data were analysed by plotting the estimated net weight gain (after correction of wettability) per unit length of circumference or per unit contact area. For simplicity, a constant “wettability” was assumed and no correction was made for the slag film between the sample and the slag. The estimated net weight gain per unit length of circumference differed considerably for three size samples, but the estimated weight gain per unit contact area was found to give reasonably close results as shown in Figure 11. This suggested that the mass flow due to penetration or dissolution was likely to be predominantly determined by the contact area, and the contribution from slag creeping was probably small. The short horizontal bars indicated the net weight gains measured from the free hanging samples after the tests, which were found to be higher than those estimated for the two smaller samples ( $\Phi 20$  and  $30$  mm) but significantly lower than that estimated for the large sample ( $\Phi 40$  mm). Use of a constant wettability and nominal circumference contact in the corrections was likely reasons for the results observed with two small samples in Figure 11. The observation for the large sample of  $\Phi 40$  mm, however, could not be explained by this, or attributed to other experimental uncertainties. The unexpected behaviour was likely to be caused by interference due to surface tension, i.e., when the gap between the sample and the crucible narrowed (the crucible was slightly tapped towards the bottom).

For the addition of 5 wt%  $\text{FeO}_x$  to the slag (Figure 3), the net weight gain was also estimated and shown in Figure 12. The estimated net weight gain was slightly higher than that measured at the end of the experiment, probably due to experimental uncertainties and the un-corrected contribution from the slag film formed between the slag and the refractory sample. As the weight gain was the net effect of the penetration and dissolution, the increase in the penetration due to 5 wt%  $\text{FeO}_x$  addition was greater than that shown in Figure 12. The significantly enhanced (and prolonged) penetration likely resulted from increased wetting and possible preferential reactions between iron oxide and periclase and spinel grains inside the refractory.

Also shown in Figure 12 are the estimated penetration (per contact area) of the calcium ferrite slag into the magnesia and magchrome refractories. Although the slags involved differed considerably, the results nevertheless clearly indicate the strong effect of iron oxide on the wetting and penetration of molten slags into magnesia based refractories. Significantly enhanced penetration for the calcium ferrite slags was likely due to increased wettability ( $> 500 \text{ dyn cm}^{-1}$  compared with  $< 430 \text{ dyn cm}^{-1}$ ) and much lower kinematic viscosity (about  $5 \times 10^{-2}$  compared with  $3 \text{ cm}^2 \text{ s}^{-1}$ ).

#### *D. Kinetics of Slag Penetration*

Slag penetration in porous refractories is determined by a range of factors including interfacial properties, slag chemistry, and structural characteristics of refractories. In principal, the driving force for slag penetration is due to wetting and capillary effects. The motion of liquid rise in a capillary of radius,  $r$ , is closely described by the following equation<sup>[16,17]</sup>

$$h \frac{dh}{dt} = \frac{r^2}{8\eta} \left( \frac{2\gamma \cos \theta}{r} - \rho g h \right) \quad (2)$$



where  $h$  is the height of liquid rise in the capillary,  $g$  the gravitational acceleration,  $\eta$  and  $\rho$  are the viscosity and density of the liquid, respectively. For a horizontal capillary, the equation becomes:

$$h \frac{dh}{dt} = \frac{r\gamma \cos\theta}{4\eta} \quad (3)$$

and a simple solution could be readily derived as

$$h = \sqrt{\frac{r\gamma \cos\theta}{2\eta} t} \quad (4)$$

Eq (4) also applies to the initial capillary rise in a vertical tube over a short period (when  $h$  is very small and thus the second term in the bracket in Eq 2,  $\rho gh$ , can be neglected).<sup>[18,19]</sup>

In order to apply these equations to liquid penetration in a porous solid, assumptions are often made that the porous solid be treated as a bundle of infinitive parallel capillary tubes of the same radius.<sup>[19,20]</sup> Apparently, this assumption is rarely valid in reality, as the three dimensional pore structure in porous refractories is extremely complex and, in many cases, this is further complicated by reactions between penetrated slag and refractory grains.<sup>[16]</sup>

Taking the silicate slag and magnesia spinel refractory as an example, the depth of initial penetration at 4 seconds could be estimated from Eq (1) to be about 0.83 mm, based on an apparent porosity of 18 % for the refractory, a density of 2.6 g cm<sup>-3</sup> for the slag. However, the penetration depth predicted by Eq (4) was 1.8 mm, based on a median pore radius of 3.5  $\mu$ m (measured by mercury intrusion porosimeter), a wettability of  $\gamma \cdot \cos\theta = 423$  dyn cm<sup>-1</sup>, and the a viscosity of  $\eta = 8.7$  poise.<sup>[21]</sup>

The difficulties in applying the simple models for capillary flow to complex porous media have been the subject of extensive studies. Various attempts have been made to introduce structural parameters into these equations.<sup>[17,19,22,23]</sup> However, a satisfactory quantitative solution to the problem is yet to be found and this remains an important subject for future research.

## V. CONCLUSIONS

A new gravimetric technique has been developed to provide direct information on the instantaneous processes of dynamic wetting, penetration/dissolution, and wear of the refractories by molten slags. Such information can not be conveniently obtained from existing conventional techniques.

The gravimetric results of the three model slag-refractory systems showed complex behaviours of the slag-refractory interactions, from simultaneous penetration and dissolution, predominant penetration with little dissolution, to severe penetration/cracking and refractory failure due to slag attack.

The slag penetration was generally non-uniform and could be very complex in some slag-refractory systems. The rate was determined by slag-refractory interfacial properties, slag properties and chemical and structural characteristics of the refractories. The reactions between

the penetrated slag and the refractory grains played an important role as demonstrated by penetration of the calcium ferrite type slag into the magchrome refractory.

Gravimetric data could be analysed to provide quantitative information on wetting and penetration/dissolution of refractories by molten slags:

- Wettability, defined as  $\gamma \cdot \cos\theta$ , could be estimated from the gravimetric data and the values derived were in good agreement with literature data.
- The amount of slag penetration could be readily calculated if the dissolution of the refractory was small, or alternatively, the net weight change due to simultaneous penetration and dissolution could be estimated from the gravimetric data.
- Iron oxide in the slag had a significant effect on wetting and penetration of magnesia based refractories, because of its influence on the wettability and the kinematic viscosity of the slags.
- The wettability of calcium ferrite slags on the magchrome refractory is poorer than on the magnesia refractory. Rates of slag penetration in the two refractories, however, are similar due to comparatively higher porosity and larger pore size in the magchrome refractory.

## ACKNOWLEDGMENT

Financial support for this was provided by the Australian Government Cooperative Research Centres Program through the G K Williams Cooperative Research Centre for Extractive Metallurgy, a joint venture between the CSIRO Division of Minerals and the Department of Chemical Engineering, The University of Melbourne. The authors wish to thank Dr Colin Nexhip for his help in early experimental trials.

## Reference List

1. M. Kobayashi, M. Mishi and A. Miyamoto: *Taikabutsu Overseas*, 1982, 2(2), 5.
2. W. Lee and S. Zhang: *International Materials Reviews*, 1999, 44(3), 77.
3. W. E. Lee, P. Korgul, K. Goto and D. R. Wilson: Adv. Refract. Metall. Ind. II, Proc. Int. Symp., 1996, pp. 453-465.
4. K. Yamaguchi, F. Ogino and E. Kimura: *EPD Congress*, 1994, 803.
5. R. Crescent and M. Rigaud: Proc. Int. Symp. Adv. Refract. Metall. Ind., 1988, pp. 235-50.
6. K. Sugita: ISR'98, J. Wang et al, 1998, p. 9.

7. K. Mukai, J. M. Toguri, N. M. Stubina and J. Yoshitomi: *ISIJ International*, 1989, 29(6), 469.
8. K. Mukai: *Phil. Tran. Royal Soc.*, 1998, 356, 1015.
9. Z. Tao, K. Mukai and S. O. M. Yoshinaga: *PacRim2*, 1996, pp. 23-28.
10. P. R. Childambaram, G. R. Edwards and D. L. Olson: *Metall. Trans.*, 1992, 23B, 215.
11. R. Benesch, R. Knihnicki and J. Janowski: *Arch. Hutn.*, 1976, 21(4), 591.
12. V. D. Eisenhuttenleute: *Slag Atlas*, Verlag Stahleisen GmbH, Germany, 1995.
13. J. Henderson: *Trans. AIME*, 1964, 230, 501.
14. R. I. Gulyaeva, S. H. Shin, P. A. Kuznetsov and A. I. Okunev: *Melts*, 1990, 4(2), 80.
15. Y. Wanibe, S. Yokoyama, T. Itoh, T. Fujisawa and H. Sakao: *Tetsu-To-Hagane*, 1987, 73(3), 491.
16. S. Zhang and A. Yamahuchi: *J. Ceramic Soc. Japan*, 1996, 104, 83.
17. Y. Wanibe, H. Tsuchida, T. Fujisawa and H. Sakao: *Trans ISIJ*, 1983, 23, 322.
18. J. Ligenza and R. B. Bernstein: *J Am Chem Soc.*, 1951, 73, 4636.
19. K. Semlak and F. N. Rhines: *Trans. AIME*, 1958, 212, 325.
20. G. P. Martins, D. L. Olson and G. R. Edwards: *Metall. Trans.*, 1988, 19B, 95.
21. J. S. Machin and T. B. Yee: *J. Am. Ceram. Soc.*, 1954, 37, 177.
22. R. B. Bhagat and M. Singh: modeling of infiltration kinetics for the in-situ processing of inorganic composites, in *In-Situ Composites: Science and Technology*, Minerals, Metals and Materials Soc., 1994, p. 135.
23. Y. Wanibe, S. Yokoyama, T. Fujisawa and H. Sakao: *Process Technology Proceedings*, 1986, 6, 911.

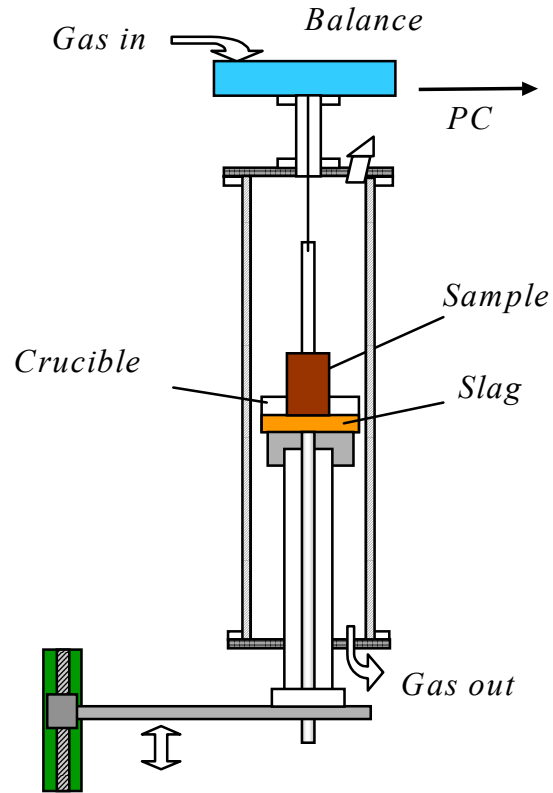


Fig. 1 Schematic diagram of experimental arrangement.

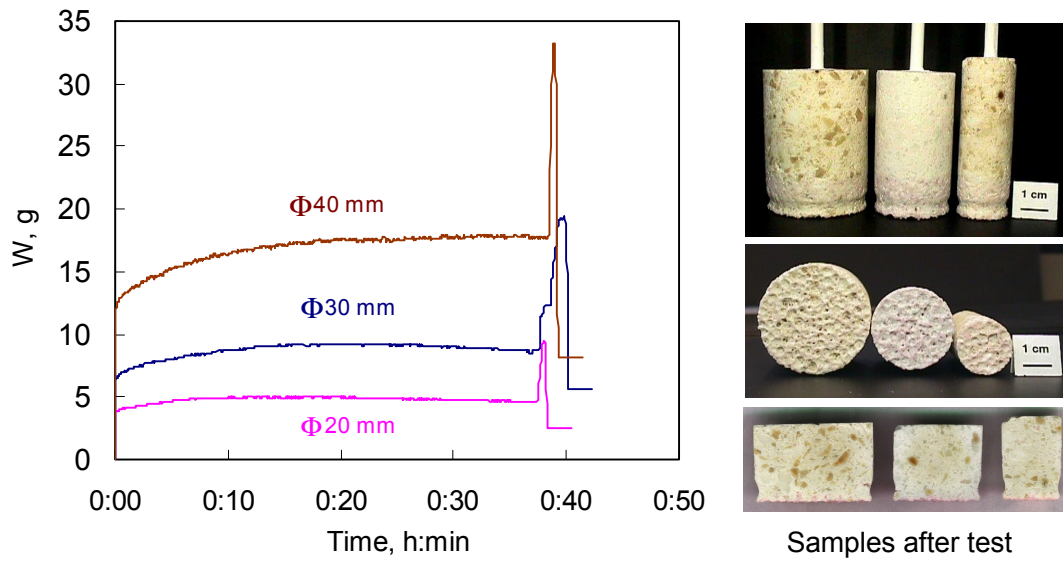


Fig. 2 Gravimetric curves for the magnesia spinel refractory in contact with the silicate slag at 1500°C under argon and the refractory samples after the test.

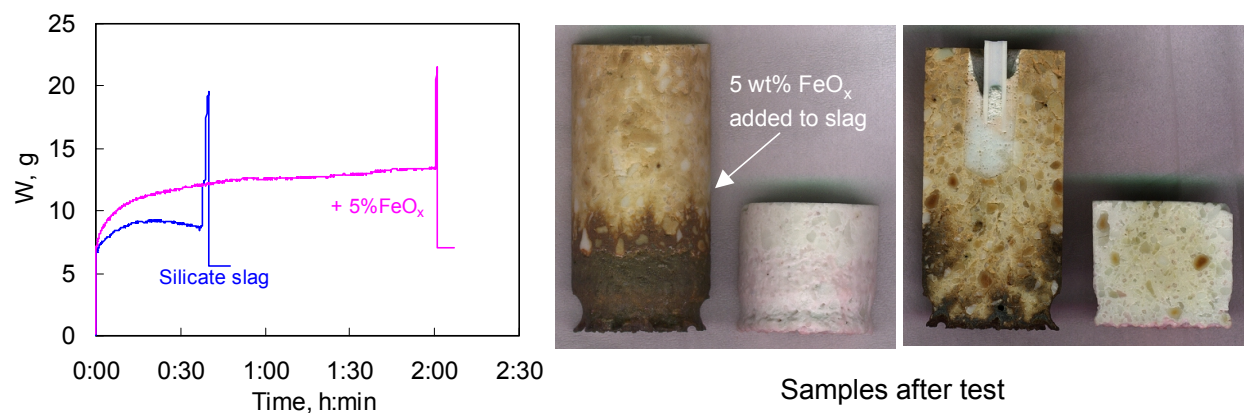


Fig. 3 Gravimetric curves showing effect of adding 5 wt% FeO<sub>x</sub> on the penetration of the silicate slag into the magnesia spinel refractory (sample  $\Phi$ 30 mm, 1500°C, argon) and the refractory samples after the test.

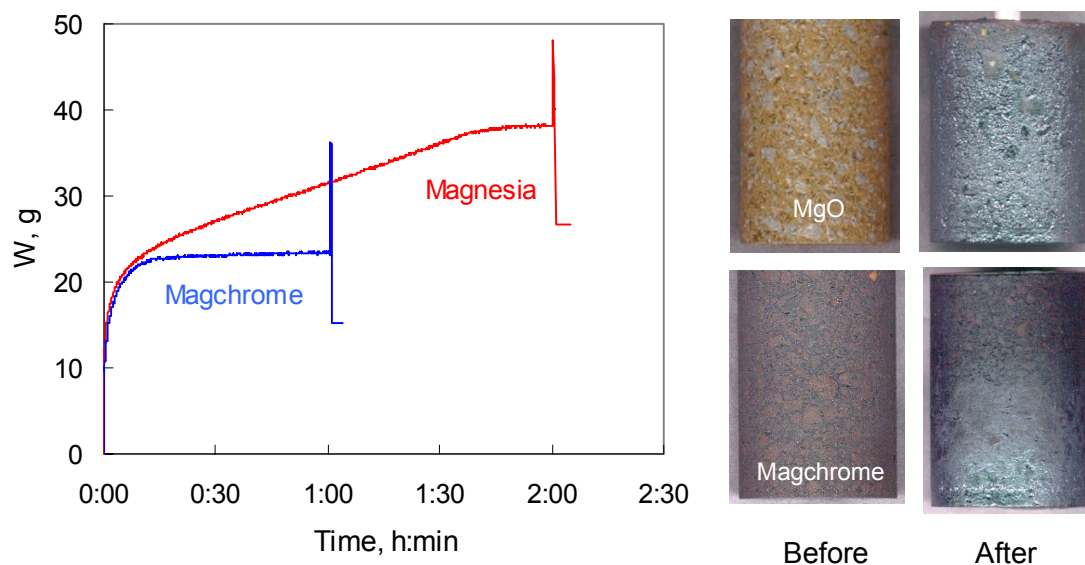


Fig. 4 Gravimetric curves for the magnesia and magchrome refractories in contact with the calcium ferrite slag at 1300°C and  $pO_2=10^{-6}$  atm (sample  $\Phi$ 30 mm) and the refractory samples before and after the test.

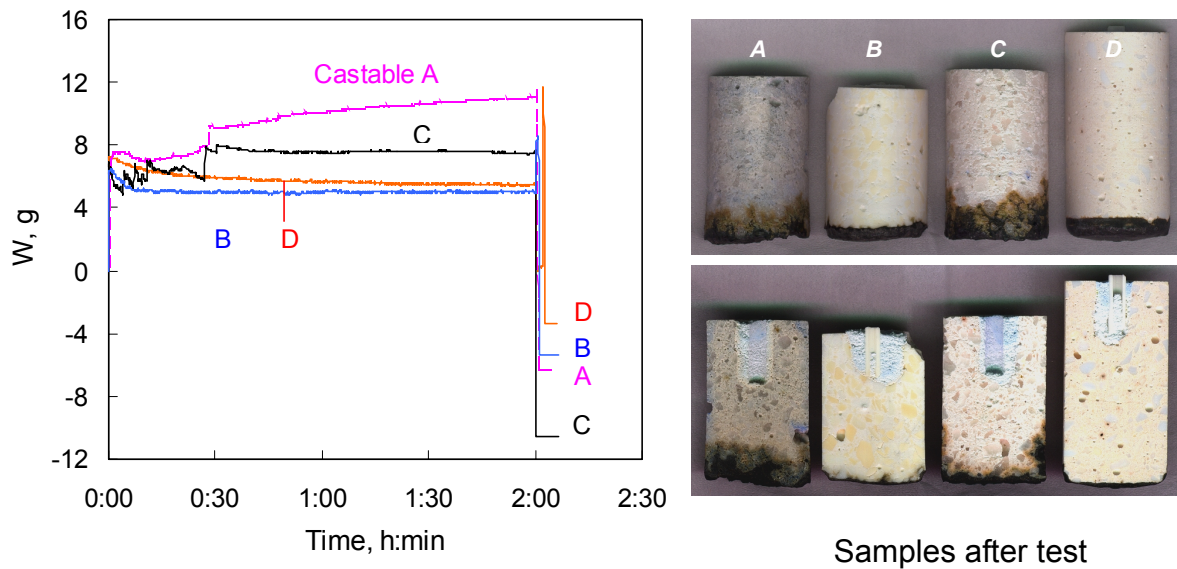


Fig. 5 Gravimetric curves showing interactions between the alumina castable refractories and the ladle slag at 1600°C under argon atmosphere (refractory sample  $\Phi 30$  mm) and the refractory samples after the test (original sample length in mm, A = 52.3, B = 45.7, C=54, D=60.4).

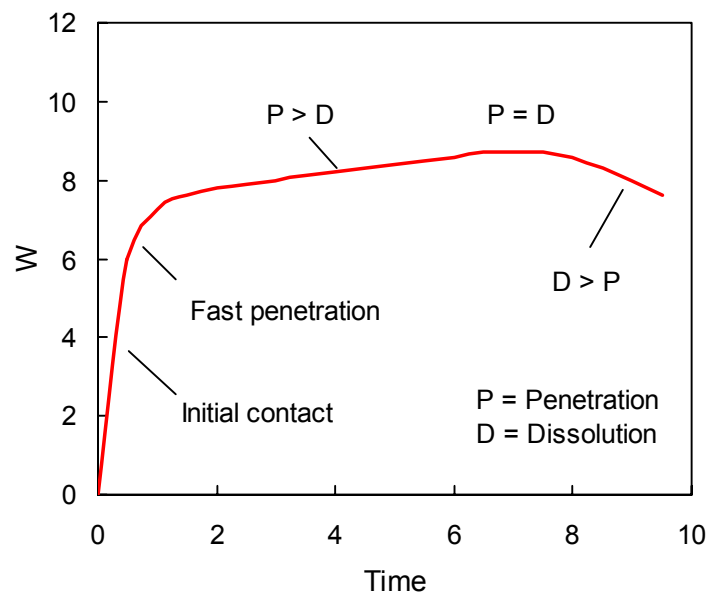


Fig. 6 Conceptual interpretation of a typical gravimetric curve.

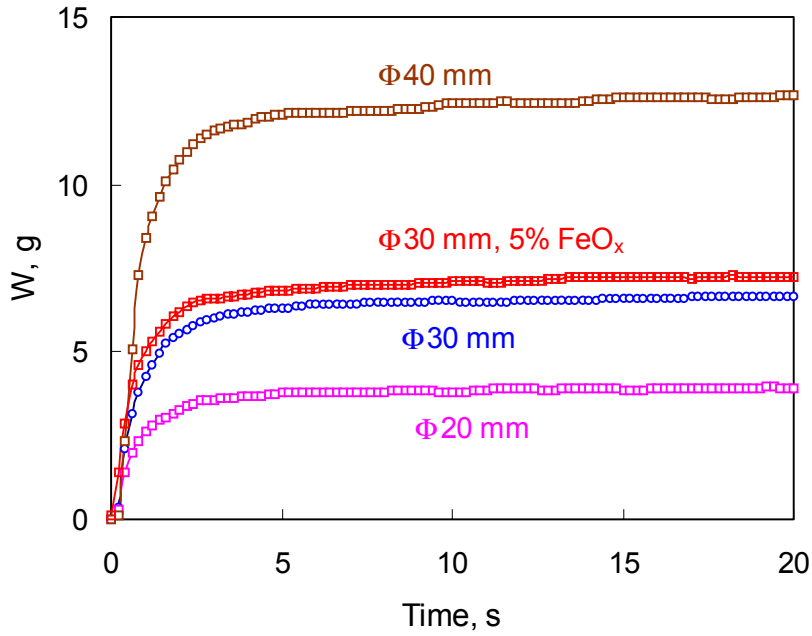


Fig. 7 Weight changes during initial contact between the magnesia spinel refractory and the silicate slag.

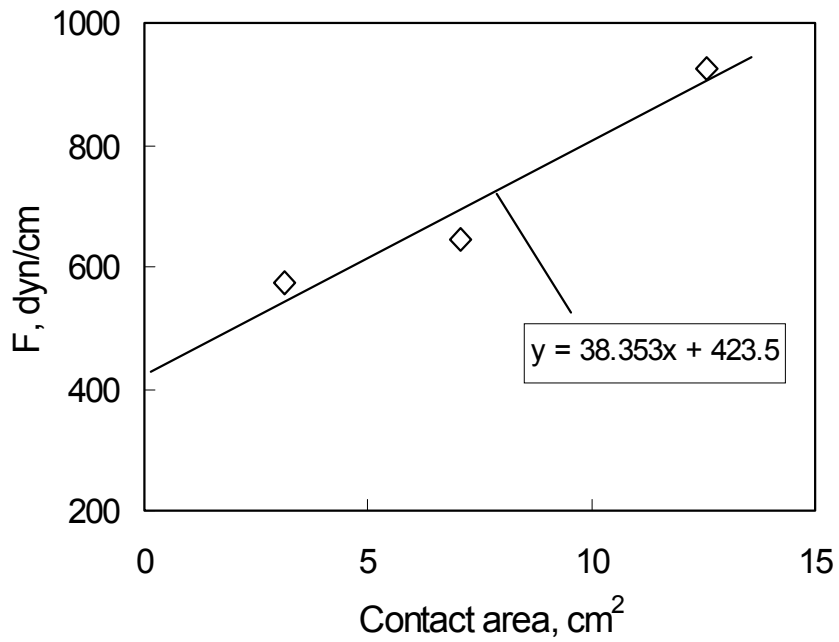


Fig. 8 Effect of contact area on wetting force per unit circumference,  $F$ , at  $t = 4$  sec contact between the magnesia spinel refractory and the silicate slag.

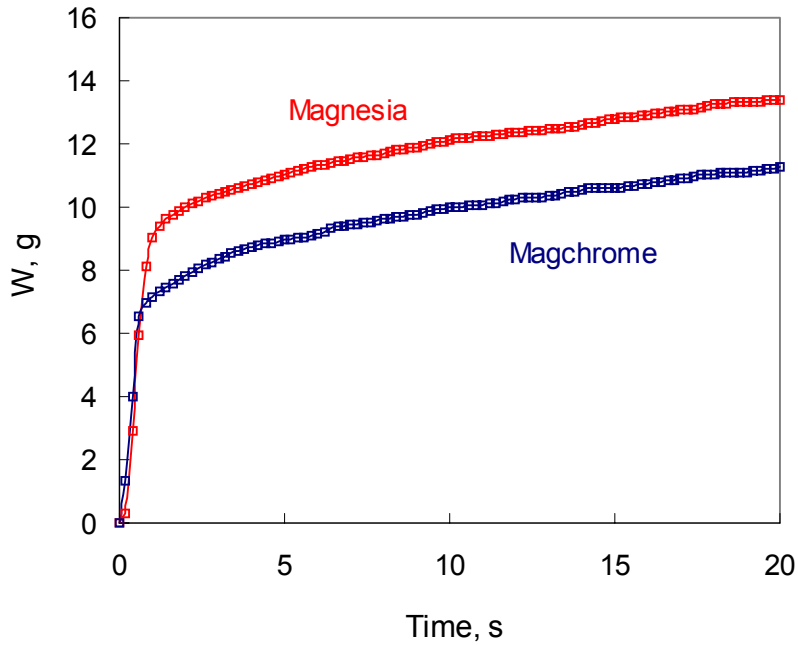


Fig. 9 Weight change during initial contact between the calcium ferrite type slag and the magnesia and magchrome refractories.

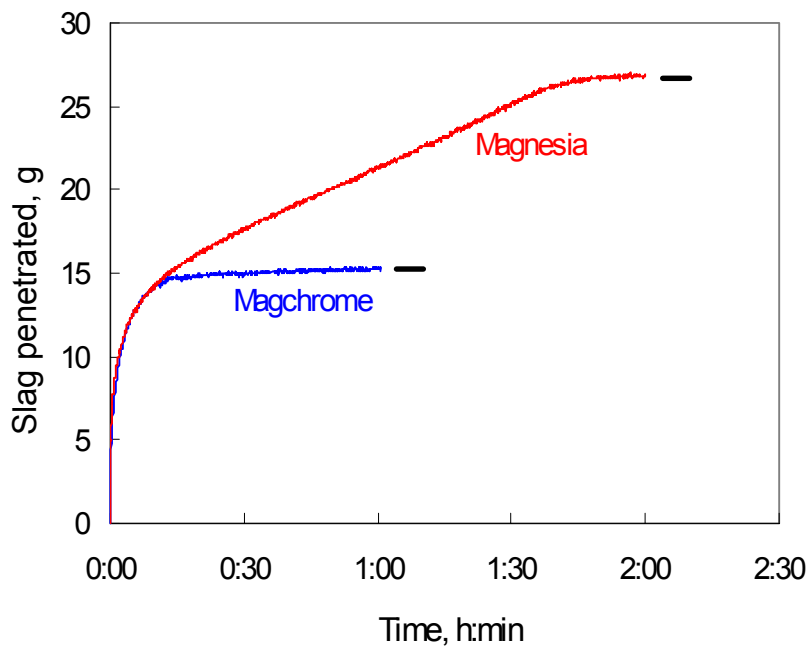


Fig. 10 Estimated amounts of the calcium ferrite slag penetrated into the magnesia and magchrome refractories. The short horizontal bars show the actual weight gain measured from the free hanging refractory samples after the test.



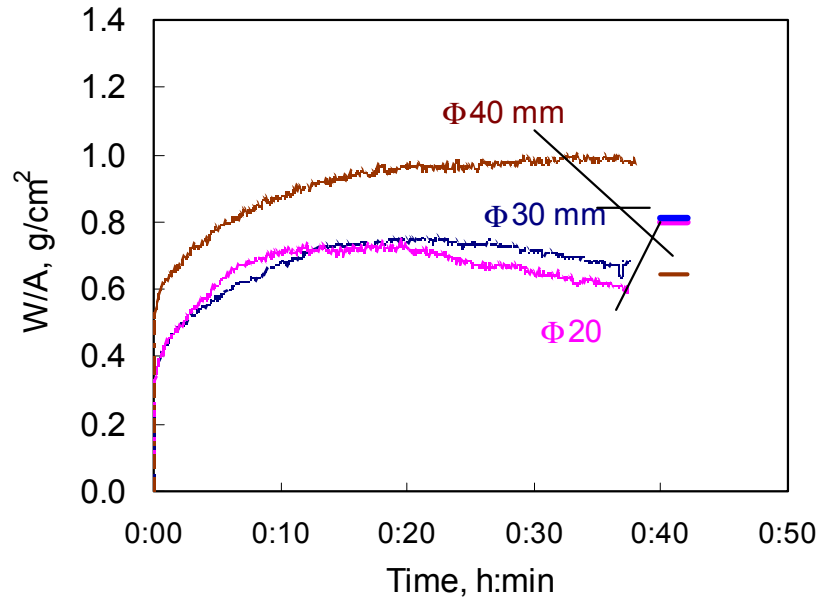


Fig. 11 Estimated net weight gain per unit contact area for the magnesia spinel refractory in contact with the silicate slag at 1500 °C. The short horizontal bars show the measured net weight gain at the end of the test.

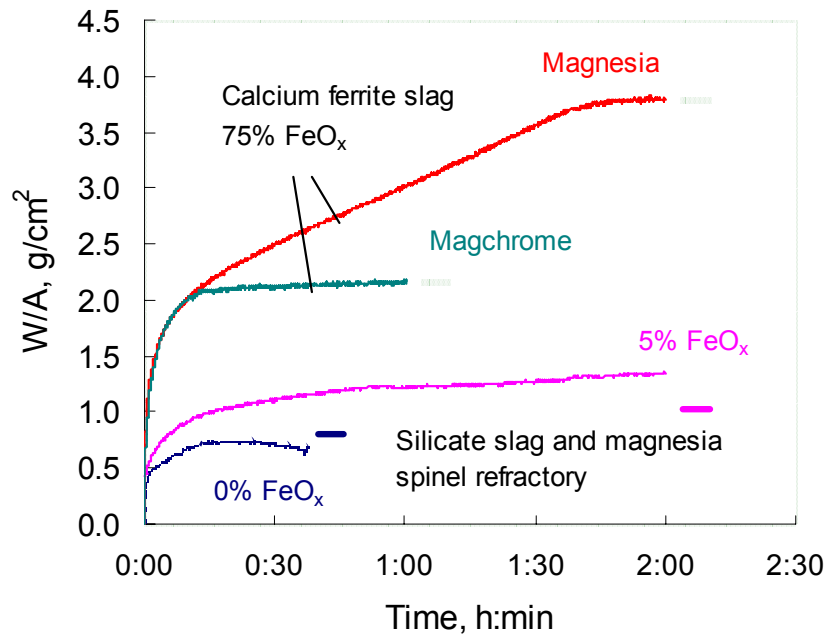


Fig. 12 Effect of 5 wt%  $\text{FeO}_x$  addition on the estimated net weight gain of the magnesia spinel refractory in contact with the silicate slag at 1500 °C, in comparison with the estimated penetration of the calcium ferrite slag into the magnesia and magchrome refractories at 1300°C and  $p\text{O}_2=10^{-6}$  atm. The short horizontal bars show the measured net weight gain at the end of the test.

Table 1 Compositions (wt%) of the silicate slag and the magnesia spinel refractory

	SiO <sub>2</sub>	CaO	Al <sub>2</sub> O <sub>3</sub>	MgO
Slag	42	28	20	10
Refractory	0.2	0.9	6.5	92

Table 2 Compositions (wt%) of the calcium ferrite type slag and the magnesia and magchrome refractories

	Fe <sub>2</sub> O <sub>3</sub>	MgO	Cr <sub>2</sub> O <sub>3</sub>	SiO <sub>2</sub>	CaO	Al <sub>2</sub> O <sub>3</sub>	Cu <sub>2</sub> O
Slag	75.7				19.4		5.3
MgO refractory		95		2.0	2.3	0.1	
Magchrome		52.5	23.55	1.42	0.71	12.6	

Table 3. Compositions (wt%) of the ladle slag and the alumina castable refractories

	Al <sub>2</sub> O <sub>3</sub>	CaO	SiO <sub>2</sub>	MgO	Fe <sub>2</sub> O <sub>3</sub>	MnO
Slag	25.0	42.0	12.0	10.0	6.0	5.0
Castable A	85.4	2.1	2.2	8.5	0.5	
Castable B	91	0.6	2	3.2	0.01	
Castable C	92.8	1.7	0.1	4.9		
Castable D	93		0.3	3.2	0.2	